Investigation of DC and AC Energy Transfer Transients for Ultra Deep Wells

Pavol Rafajdus[1], Vladimír Vavrúš[1], Jozef Kúdelčík[1] and Branislav Dobrucký[1]

[1] Faculty of Electrical Engineering, University of Žilina, Slovakia, e-mail: *pavol.rafajdus@fel.uniza.sk*

Abstract — **This paper deals with the investigation of DC and AC energy transfer transients for ultra deep wells. Two transfer energy approaches are described: DC and AC three phase systems transmission via power cable. The transients could be switch on, switch off for no load, rated load and over load conditions. The simulations analysis of both systems are described and compared. The losses are calculated and discussed.**

Keywords — energy transfer for ultra deep wells, DC and AC transient analysis

I. INTRODUCTION

This paper deals with energy transfer systems to obtain geothermal energy. At this time, the renewable sources of energy are split of water, wind, solar, bio fuels and geothermal. As it is known, temperature of water under Earth in the depth of around 10 km is about 200 °C under 95 % of the Earth's surface. At the present, used technologies for wells are based on mechanical destruction of rock. The depth is from 3 to 5 km and it arises from crude oil production cases. In some places as Iceland, there is temperature of water around 600 °C and it is max. 5 km under ground. For very deep wells the price is very high and expensive to obtain energy from geothermal sources [1], [4].
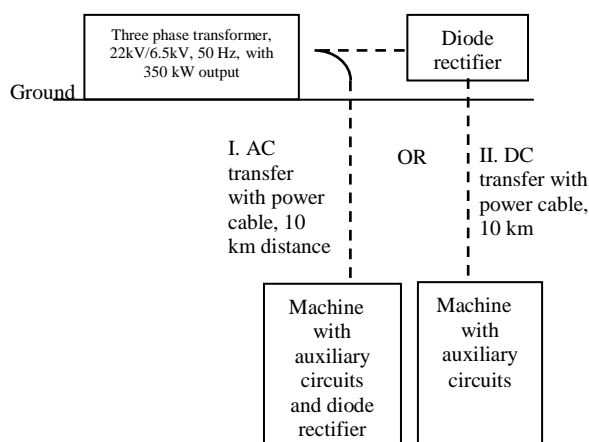

Fig. 1: The block diagram of the machine structure with AC or DC energy transfer

This paper deals with the energy transfer from a power source which supplies machine for ultra deep wells up to 10 km for the AC and DC transfer system

Very simple block diagram of the machine structure is shown in Fig. 1. There can be seen two possible conceptions of the energy transfer. The first is the AC transfer, where a power transformer or other power source is located at the ground and the diode rectifier is in the well. This approach is described in chapter III. from point of view of some transients as switched on, switched off, no load or short circuit load conditions. The second approach is the DC transfer, where the diode rectifier is located at the ground. This analysis is shown in chapter II. Both approaches are compared and some recommendations are given.

Regarding of over-voltages in energy transfer system

Generally, in electric circuit include: aerial power high voltage (hv) lines – transformer – power supply by hv cable – hv rectifier – load (plasma system). There may occur several types of over-voltages:

- atmospheric over-voltages,
- commutation over-voltages,
- switching over-voltages.

This paper in the later text deals just with switching over-voltage produced during disconnect of the rectifier inductive load (plasma system). The magnitude of the over-voltage is proportional to the current magnitude at the instant of interruption as well as to decreasing of interruption (time of switch-off, responding time of electronic protection, extinguishing the plasma discharge in the plasma system ...).

Beyond that, however, it will also depend on the surge magnitude caused by other factors:

- power cable length, respectively, on its accumulated energy
- internal impedance of the power supply, if it is not disconnected during circuit interruption,
- an instant of the load circuit disconnection in the range of rectifier output voltage period i.e. one sixth period of the AC power supply voltage period 50 Hz (i.e. in the range of 0-3.3 msec.).

In our case, it is supposed the power supply is disconnected at the same time as the load comes off

plasma system. It is necessary to ensure the release of the power supply high-speed switch with trip response time shorter than the period of the increased voltage at the end of the transmission cable limit (allowable surge), what is not a simple matter.

To limit the magnitude of the over-voltage surge safely it is necessary to use a short-circuit switch, best of an electronic type. When the over-voltage reach a critical value (7 500 V) electronic switch – thyristor will switch-on the short circuit, Fig. 2.
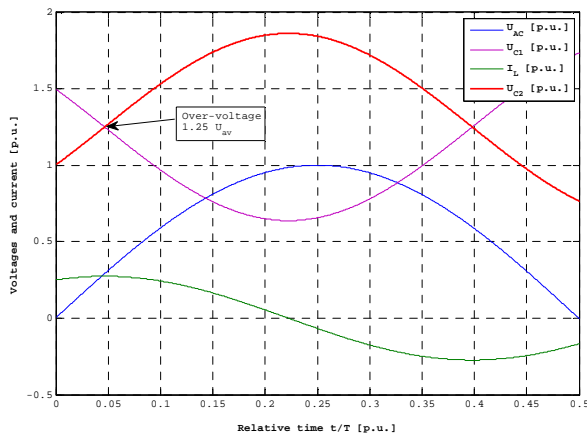

Fig. 2: Illustrative over-voltage of 7500 V at 1 ms after load switch off

II. DC TRANSFER SYSTEM

The simulations of the power cable properties were made using direct current circuits. The advantage of these direct current circuits is the possibility to predict the performance of the electrical system. Using of these circuits and their combinations can describe all situations, which can occur in real wires of the power cable. At the present time the first step of evolution of a new equipment is simulation process, which safes money and time. From the results of simulations it is selected the best one, which is then realized.

The program LTSpice was used for simulation of the power cable properties and its transient stages. The simulated circuit (Fig. 3) consists of the DC source (6400 V) with series resistor (1 mΩ), two or three programmable switches, ten alternative Π-circuits and RL load. Alternative Π-circuit is used in practice and satisfies all conditions for our type of real wires of the power cable. On the knowledge from practices, the power cable has been replaced by 10 alternative Π-circuits. The switch S2 disconnected the RL load form the power cable. The load was performed as RL circuit (L = 1 mH and R = 103 Ω). The value of the resistance R is set to load of 350 kW.

A short-circuit thyristor is also used in the circuit. The short-circuit thyristor is represented by the switch S1 together with the inductance 20 μH and resistor 480 mΩ in series (Figs. 3, and 5). It is placed at the end of the power cable. The shorting voltage of the thyristor was set to 7 500 V. We studied two cases: A. short circuit at the output cable and disconnection of the DC source and B. short circuit at the input and output of the cable and disconnection of the DC source.

A. Short circuit at the output of the cable and disconnection of the DC source

The simulation of the disconnection of RL load was realized in several steps. In first 5 ms the output at the end of the cable was stable and with the value of 6 kV. Using the switch S2 in 5 ms the RL load was disconnected. Immediately after then the voltage began rise to big values. 7 500 V was achieved in 50 μs and S1 and S3 (Fig. 3) were switched in this time (5.05 ms). S1 - thyristor shorted the end of the power cable and S3 disconnected the DC source. The development of the voltage and current are shown in Fig. 4.
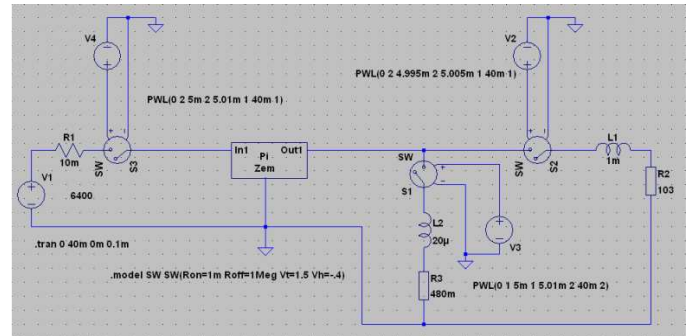

Fig. 3: The diagram of the simulation circuit with DC source, 10 Π-circuit, programmable switches S1-S3, short-circuit thyristor and RL load.

Development of changes of current and voltage at the first Π-circuit or the input of the power cable after 5 ms is shown in Fig. 4. The current (red curve) decreases to zero immediately but for the voltage (black curve) there are big overshoots of the voltage (15 kV). The response time for the voltage is short because the amplitude of these overshoots is smaller than 6 kV after 4 ms. In our previous work [1] we had similar situation. We can conclude that this type of solution is also bad; the voltage amplitude oscillation is too high.
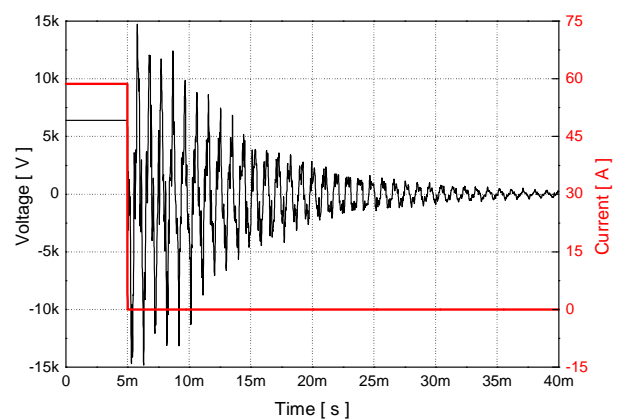

Fig. 4: Development of the voltage at the first of Π-circuit (start of power cable) after disconnection of the RL load in 5 ms.

B. Short circuit at the input and output of the cable and disconnection of the DC source

The simulation of the disconnection of the RL load was in this case also realized in 5 ms after beginning of the simulation. When the RL load was disconnected, the

voltage began to rise from 6 000 V to higher voltage. 7 500 V was achieved in 50 µs and S1, S4 and S3 (Fig. 5) were switched in the simulation time equal to 5.05 µs. S1 - thyristor shorted the end of the power cable, S4 shorted the start of the power cable and S3 disconnected the DC source. The development of the current and voltage are shown in Figs. 6 and 7.
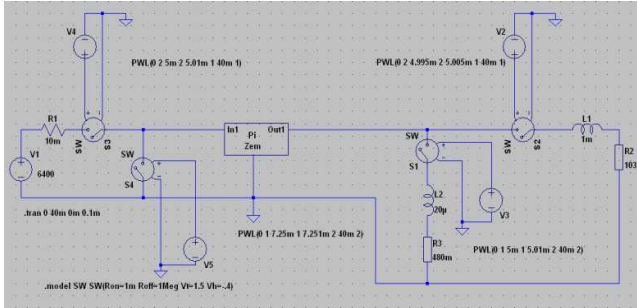

Fig. 5: The diagram of the simulation circuit with DC source, 10 Π-circuit, programable switches S1-S4, short-circuit thyristor and RL load.

Developments of the measured parameters are in this case better than in the previous case A (Fig. 4). The instantaneous voltage drop to zero is caused by shorting of the power cable at the beginning (Fig. 5, switch S4). The amplitude of current oscillations is ~120 A and duration is about 20 ms (Fig. 6). Observed current oscillations are much better than the over-voltage shown in Fig. 4.
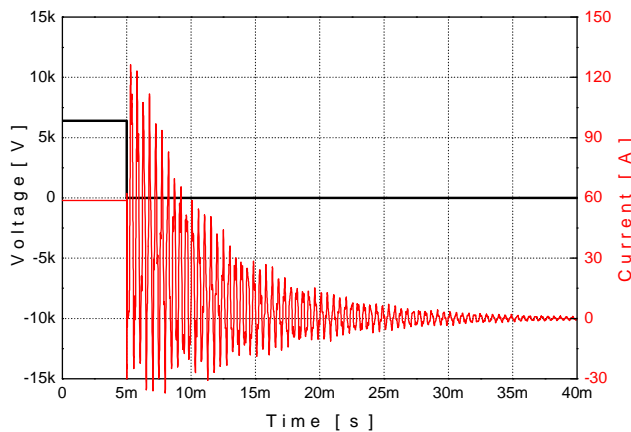

Fig. 6: Development of the voltage at the first of Π-circuit (start of power cable) after disconnection of RL load in 5 ms.

Another situation is at the end of the power cable (Fig. 7). The voltage decreases from 7 500 V to zero with small oscillations during 350 µs. The amplitude of current oscillations is ten times higher as normal current. This is no problem for thyristor because its max current is around 1.2 kA and the transient time is only 0.4 ms. In next 7 ms, the amplitude of next oscillation decreases from 150 A to 60 A. From these simulations of transient states results that our design of the RL load disconnection presented in Fig. 5 is better.

I. AC TRANSFER SYSTEM

AC voltages are useful and more efficient for supplying long distance distribution power lines. Simulation results, described below, show transients analysis results of the over-voltage protection.
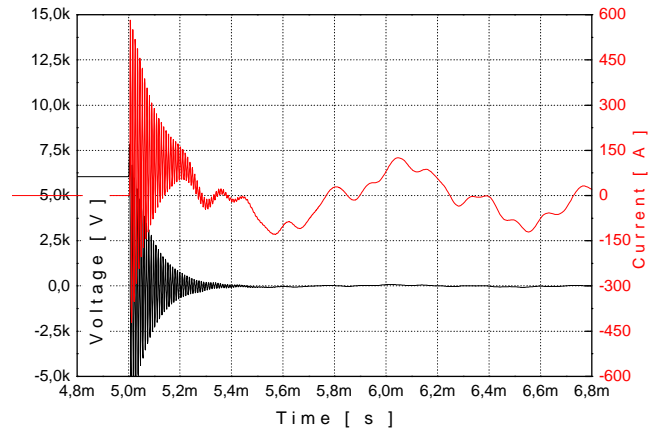

Fig. 7: Development of the voltage at the end of the power line and the current flows through the thyristor at disconnection of the RL load in 5 ms.

The RL load is powered by the 6 kV DC voltage with total power of 350 kW. The simulation model consists of controlled AC voltage source, investigated 10 km long power cable line, bridge rectifier, DC bus filter devices, over-voltage protection devices and load. The DC bus circuit diagram is showed in Fig. 8. At the power cable start there are series connected power switch and parallel connected cable breaker. Voltage and current meters are at the input and output of the power cable, the DC bus and load are required. The DC bus voltage is filtered by the C_f capacitor with 50 µF value and the current is filtered by the L_f inductance with 1 mH value. Over-voltage stress is generated by suddenly disconnection of the load through the load power switch.
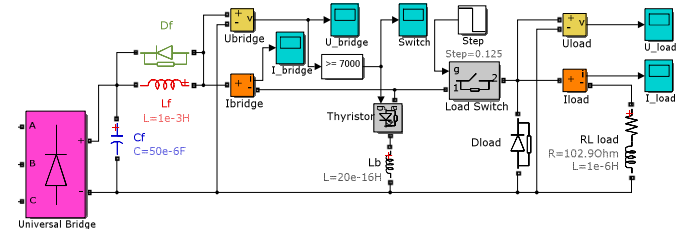

Fig. 8: DC bus circuit diagram

Over voltage protection devices consist of the series connected breaking thyristor and current peak limiting inductance with 20 µH value. After disconnecting the load (load current cannot be conducted again) over voltage peak is generated in the DC bus. This voltage is measured and compared with a user defined value (protection trip voltage) and the exceeding is turned on the DC bus breaking thyristor, the cable input breaking switch and turned off the cable input switch. In the real application it can be used one high voltage thyristor or series connected medium voltage thyristors as the DC bus breaking switch [7]. Acting times of these switching devices are very short, so simulation model also uses model of the thyristor as breaking device. However, cable input protection switches should by electromechanical switches. Acting time of the electromechanical switches is not too quick, so the over-voltages and currents peaks can affect system protection results. The upgraded simulation model respects these conditions by added time delay between the DC bus thyristor turn-on time and the cable input switches turn-on (turn-off for the input power source switch) time. The time delay is defined for high speed high power switches and it is set to 2 ms. Results without the time

delay block between the input and DC bus were published in [8]. The voltages and currents relation for a 3-phase power cable are investigated.

A. 3-phase AC power analysis

Investigated over-voltage stress analysis used the 3-phase cable model. For this simulation, new cable parameters are measured. Principles of parameters measuring are discussed in [2]. Used power cable parameters are shown in table II.

TABLE I. 3-PHASE CABLE PARAMETERS

Parameter	Values			Unit
	Phase A	Phase B	Phase C	
Frequency (f)	50			Hz
Conductor self resistance per unit length (R_S)	0.604	0.596	0.595	Ω/km
Conductor self inductance per unit length (L_S)	1.968	1.984	1.803	mH/km
Per phase mutual inductance per unit length (L_M)	1.266			mH/km
Per phase mutual resistance per unit length (R_M)	12.381			mΩ/km
Line-line capacitances per unit length (C_C)	15.732	16.161	16.371	nF/km
Conductor-to-ground capacitances per unit length (C_G)	69.497			nF/km
Cable length (l)	10			km
Number of Pi sections	10			-

The cable connection to the bridge rectifier is shown in Fig. 9. the load is supplied from the controlled 3-phase AC voltage source. The input voltage amplitude is linearly increased during 0.08 s and power current peaks, which are produced by the charging cable capacitances and DC bus capacitance, are then eliminated (Fig. 10 a)). The cable input switch and cable breaker are three phase devices. The cable breaker makes direct connection between each phase and ground too.
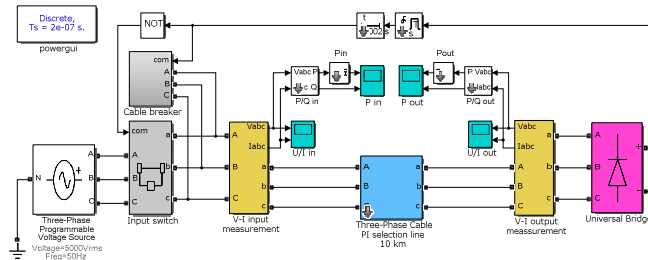

Fig. 9: 3-phase power cable bridge rectifier connection with delayed input stages

Amplitude of the input voltage is set to a value which corresponds to the DC bus average voltage of 6 kV. The load disconnecting time is defined at the instant of the phase A maximum input voltage ($t_{off} = 0.125$ s).

After the load disconnection, the DC bus voltage is increased over the trip point set at 7 kV (Fig. 12 b)). The voltage increasing time and parameters are dependent so the breaking thyristor is turned on later after the load disconnection (Fig. 10 b)).

The input cable breaker turn-on time is delayed of 2 ms after the DC bus thyristor. The breaker makes short connection between all cable phases and ground too, so

discharging of the cable input capacitances produce current peaks in phases, voltages of which are not zero (Fig. 10 a), details are in Fig. 10 b)). Maximum value of these peaks is not higher than 600 A.
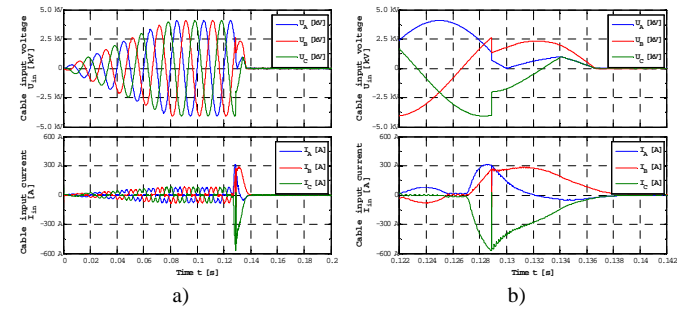

Fig. 10: Cable input voltage and current waveforms

Fig. 10 b) shows in details the cable input voltages and currents after the DC bus thyristor activating and delayed input breaker turn-on. After the thyristor is switched on, the cable is still connected to the AC power source, so voltages continue but currents are rapidly increased because the DC bus breaking thyristor short connects the DC bus terminals.

The current slope is limited by the cable self-inductance and DC bus filtering inductance L_f. The currents are increased in 2 ms when the cable input breaker is turned on and also the power supply is disconnected. After this moment, the currents and voltages at the cable input are slowly decreased due to high cable self-inductance and cable self-capacitances.
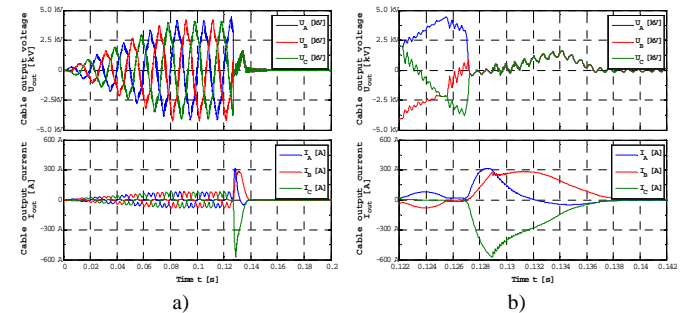

Fig. 11: Cable output voltage and current waveforms

Fig. 11 a) shows the cable output voltages and currents. As it can be seen, the cable output voltages are non-harmonic due cable parameters and non-harmonic current flowing through the cable conductors.

Acting of the breaking thyristor discharges the filtering capacitor C_f together with the cable capacitances through the filtering inductance L_f and bridge rectifier diodes (Fig. 11 b). The current response and maximum values are not critical, but the bridge rectifier diodes have to be dimensioned for these values.

Fig. 12 a) shows that, the DC bus voltage mean value is 6 kV and the voltage ripples are approximately ±300 V. The steady state DC bus current value is matched to the load parameters, respectively, load active power of 350 kW.

Activating of the DC bus thyristor produces high current peak and decreases longer time due the delayed power source disconnection.
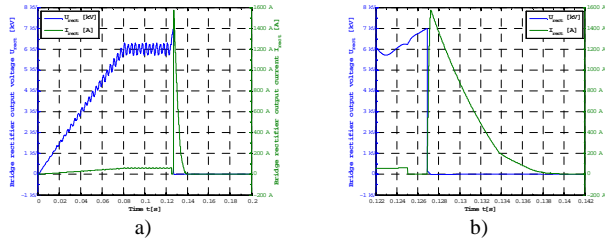
Fig. 12: Bridge rectifier output voltage and current waveforms

Higher value of energy is stored in the cable for the time of 2 ms when cable is short connected. Maximum value of the current peak is approximately 1600 A. For this maximum value the breaking thyristor and filtering inductance winding have to be dimensioned.

B. Power losses analysis

Power losses are important for the design and classification of a new devices. Losses are produced in all parts in which currents flow. For this analysis the cable power losses are investigated. Table III presents simulated values of the power losses (for fundamental frequency) of 1-phase and 3-phase cable configurations [8].

TABLE II. SIMULATED CABLE POWER LOSSES

Cable model configuration	Simulated power consumption		
	Cable input	*Cable output*	*Load*
1-phase	427.5 kW	391.2 kW	350 kW
3-phase	397.5 kW	353.8 kW	350 kW

As it can be seen, single phase cable had lower power losses (1-phase model) but 3-phase configuration is more effective (more realistic results). At the DC bus side greater power losses are produced in the bridge rectifier. Each bridge diode consists of two series connected high voltage diodes with forward voltage of 0.894 V (one diode) and internal on-state resistance of 0.48 mΩ (one diode). Also the filtering inductance reverse diode has losses, but only during the breaking time (these losses are not included in results).

It must be noted, that power transformer or power source efficiency or losses can be also included in a detail analysis (not this time). As it is known, the efficiency of such transformer is about 98 %.

II. DESIGN OF PLASMABIT DIODE RECTIFIER

A. Diode Rectifier Short-Circuit Connection

As mentioned above in the introduction for limitation of the over-voltage surge magnitude safely it is necessary to use the short-circuit switch – thyristor (SCTh), Fig. 13. Dimensions of the SCTh thyristor and the diodes of the plasmabit rectifier will depend on the overloaded integral I^2t value of the short-circuit current [1], [6].

$$I^2t = \int_0^{t_p} I_T^2\,(t)\mathrm{d}t = \frac{I_{TSM}^2 \cdot t_p}{2},$$

where I_{TSM} is the maximum non-repetitive overload current of the thyristor or rectifier diodes (I_{FSM}) and t_p

the duration of the half-sine current impulse – usually 10 ms given in catalogue data sheets . Similarly, it can be derived for the rectangular current pulse

$$I^2t = \frac{\pi^2}{4}\frac{\left(I_{TSM}^2\right)_{AV} \cdot t_p}{2},$$

that value should be less then allowed thyristor and diodes I^2t values given in catalogue data sheets (below).
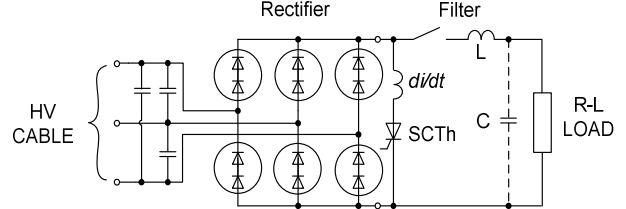

Fig. 13: Diagram of 3-phase diode rectifier with shorted-circuit thyristor SCTh

So, firstly we need to know the maximum value of the short-circuit current $I_{MAXshort\_circuit}$ for duration of 10 ms what is possible by use of simulation analysis results. This value is (worst case)

$$\left(I_{MAXshort\_circuit}\right)_{AV} = \sim 1\,700\,[\text{A}].$$

Now we can calculate $I^2t_{short\_circuit}$ value

$$I^2t_{short\_circuit} = \frac{\pi^2}{4}\frac{\left(I_{MAXshort\_circuit}^2\right)_{AV} \cdot t_p}{2} =$$
$$= 3\,566.26\,[\text{A}^2\text{sec}].$$

Choosing of a suitable thyristor from the catalogue [7] type with maximum blocking voltages (prior condition) is:
Type of 5STP 20Q8500/5STP 20N8500, $V_{DRM} = V_{RRM} = 8$ kV, $I_{TMS} = 35$ kA/10 ms, $r_T = 0{,}480$ mΩ

The calculation of the TSCTh overloading integral value is

$$I^2t_{TSCT\,h} = \frac{35\,000^2 \times 10^{-2}}{2} = 6\,125\,000\,[\text{A}^2\text{sec}].$$

By comparison of both I^2t

$$I^2t_{short\_circuit} << I^2t_{TSCT\,h},$$

i.e. that condition of operability and safety is fulfilled.

Choosing of the plasmabit rectifier diode from the catalogue [7] types with maximum blocking voltages (prior condition) gives:

5SDD 31K6000, $V_{RSM} = V_{RRM} = 6$ kV, $I_{FMS} = 40$ kA/10 ms, $V_{T0} = 0.894$ V, $r_T = 0.166$ mΩ

5SDD 06D6000, $V_{RSM} = V_{RRM} = 6$ kV, $I_{FMS} = 10.5$ kA/10 ms, $V_{T0} = 1.066$ V, $r_T = 0.778$ mΩ

That means, that 6 kV reverse voltage is not enough, so we choose series connected diodes.

Types for the series connection

5SDD 08D5000, $V_{RSM} = V_{RRM}$ = 5 kV, I_{FMS} = 12 kA/10 ms, V_{T0} = 0.894 V, r_T = 0.487 mΩ

5SDD 08T5000, $V_{RSM} = V_{RRM}$ = 5 kV, I_{FMS} = 12 kA/10 ms, V_{T0} = 0.894 V, r_T = 0.487 mΩ

The calculation of the $I^2 t_D$ overloading integral value (worst i.e. smallest value)

$$I^2 t_D = \frac{12\,000^2 \times 10^{-2}}{2} = 720\,000\,[\text{A}^2\text{sec}].$$

By comparison $I^2 t_{short\_circuit} \ll I^2 t_D$,

i.e. that condition of operability and safety is fulfilled.

B. Power Losses Calculation

Calculation of on-state losses of the single rectifier diode [1], [6]

$$\Delta P_f = \frac{1}{T} \int_0^T u_f(t) i_f(t) \mathrm{d}t = U_{T(0)} I_{fAV} + r_T I_{fRMS}^2 \quad \text{where}$$

ΔP_f is on-state Joule loss

$U_{T(0)}$ threshold voltage under zero current

I_{fAV} average value of the diode forward current

t_T transient/dynamic resistance

I_{fRMS} effective value of the diode forward current.

Average value of the output rectifier current

$$I_{outAV} = \frac{P_{outAV}}{U_{outAV}} = \frac{350\,000}{6\,000} \left[\frac{\text{W}}{\text{V}}\right] = 58.33\,[\text{A}]$$

Supposing the duration of the smoothed diode current 120 °el., the average value of the diode current will be

$$I_{fAV} = \frac{I_{outAV}}{3} = \frac{58.33}{3} = 19.44\,[\text{A}]$$

The effective (RMS) value of the diode current is

$$I_{fRMS} = \sqrt{\frac{I_{outAV}^2}{3}} = I_{outAV} \sqrt{\frac{1}{3}} = 33.50\,[\text{A}].$$

Then, considering $U_{th(0)}$ and r_t for the diode type 5SDD 31K6000 being 0.894 V and 0.166 mΩ or for the diode type 5SDD 08D5000 with 0.894 V 0.487 mΩ, respectively, the Joule loss of the single diode yields

$$\Delta P_f = 0.894 \times 19.44 + 0.166 \cdot 10^{-3} \times 33.50^2 =$$
$$= 17.38 + 0.18629 = 17.566\,\text{W or}$$

$$\Delta P_f = 0.894 \times 19.44 + 0.487 \cdot 10^{-3} \times 33.50^2 =$$
$$= 17.38 + 0.54654 = 17.927\,\text{W, respectively.}$$

The total losses of the plasmabit rectifier (two diodes in series) are

$$\Delta P_{rect} = 12 \times 17.566 = 210.792\,\text{W}$$

for the diode type 5SDD 31K6000 i.e. 6 000 V/3 097 A and 42 kA/10 ms impulse, or

$$\Delta P_{rect} = 12 \times 17.927 = 215.124\,\text{W}$$

for the diode type 5SDD 08D5000 i.e. 5 000 V/1 028 A and 12 kA/10 ms impulse. Calculated power losses should be removed from the plasmabit by a cooling system. The plasmabit rectifier diodes are overflowed/stressed by the short-circuit current of the same value as the short-circuit-thyristor. Besides of on-state losses, the diode rectifier is characterized also by commutation and switching losses (5-10 % of on-state losses/ 50 Hz). Both calculated values of the plasmabit rectifier on-state power losses and type of diodes are acceptable. Their usage and choice of one of them depends on the plasmabit space and cooling condition.

III. CONCLUSIONS

This paper presents investigation of power cable transients for novel application of the plasmabit for ultra deep geothermal wells. The real cable parameters have been investigated by means of measurements and calculations and they have been used for transient simulations. Very important decision is to choose suitable energy transfer by DC or AC supply. For this task, both are investigated by simulations of transients for connection and disconnection of the cable under load. The results are presented and compared also by using 3-phase diode rectifier for the plasmabit supplying. In the future more detail transients will be analyzed and compared.

REFERENCES

[1] B. Dobrucký, J. Kúdelčík, V. Vavrúš, P. Rafajdus, "Transient Analysis of Power Cable for Ultra-Deep Geothermal Wells", Proc. of the XII. Int'l Conf. on Low Voltage Electrical Machines, Brno-Šlapanice (CZ), CD

[2] G. Skibinski, R. Tallam, R. Reese, B. Buchholz, R. Lukaszewski, "Common Mode and Diferential Mode Analysis of Three Phase Cables for PWM AC Drives" Conference Record of the 2006 IEEE Industry Applications Conference. Vol. 2, 2006, pp. 880-888.

[3] N. Stamnes, J. Zhou, G.-O. Kaasa, O.M. Aamo, "Adaptive Observer Design for the Bottomhole Pressure of a Managed Pressure Drilling System", Proc. of the 47th IEEE Conference on Decision and Control Cancun, Mexico, Dec. 9-11, 2008, pp. 2961-2966.

[4] http://www.geothermalanywhere.com/

[5] The MathWorks, Inc. , "SimPowerSystems™ - PI Section Line Help".

[6] F. L. Huo, H. Ye, "Power Electronics: Advanced Conversion Techno-logies, " Boca Raton: CRC Press, Taylor&Francis Group, 2010, pp. 29–64.

[7] *"High Power Semiconductors Catalogue"*. ABB Switzerland Ltd., Semiconductors, Lenzburg (CH), 2013, pp. 8-11, 15-16, 18-23., 24.

[8] P. Rafajdus, V. Vavrúš, J. Kúdelčík, B. Dobrucký: "Analysis Over-voltages and Losses of Energy Transfer for Ultra Deep Wells", XX. International Symposium On Electric Machinery, ISEM 2013, Prague, Czech Republic, 2013, 09, 10.-12., pp. 71-78